Optical Materials 107 (2020) 110018

Contents lists available at ScienceDirect

Optical Materials

journal homepage: http://www.elsevier.com/locate/optmat

Spectroscopic study of Nd^{3+} ion-doped Zn-Al-Ba borate glasses for NIR emitting device applications

M. Djamal [a,b,*], L. Yuliantini [a], R. Hidayat [a], N. Rauf [c], M. Horprathum [d], R. Rajaramakrishna [e], K. Boonin [e,f], P. Yasaka [e,f], J. Kaewkhao [e,f], V. Venkatramu [g,h], S. Kothan [i,**]

[a] Department of Physics, Faculty of Mathematics and Natural Sciences, Institut Teknologi Bandung, Bandung - 40132, Indonesia
[b] Physics Study Program, Department of Science, Institut Teknologi Sumatera, Lampung - 35365, Indonesia
[c] Department of Physics, Faculty of Mathematics and Natural Sciences, University of Hasanuddin, Makassar - 90245, Indonesia
[d] Optical Thin-Film Laboratory, National Electronics and Computer Technology Center, Pathumthani - 12120, Thailand
[e] Department of Post Graduate Studies & Research in Physics, The National College, Jayanagara, Bengaluru - 560070, India
[f] Center of Excellence in Glass Technology and Materials Science (CEGM), Nakhon Pathom Rajabhat University, Nakhon Pathom - 73000, Thailand
[g] Department of Physics, Yogi Vemana University, Kadapa - 516 005, India
[h] Department of Physics, Krishna University Dr. MRAR PG Centre, Nuzvid - 521 201, India
[i] Center of Radiation Research and Medical Imaging, Department of Radiologic Technology, Faculty of Associated Medical Sciences, Chiang Mai University, Chiang Mai - 50200, Thailand

ARTICLE INFO

Keywords:
Borate glass
Neodymium
Judd-ofelt theory
Luminescence
IR emitting Material

ABSTRACT

Trivalent neodymium (Nd^{3+}) -doped Zn-Al-Ba borate glasses of composition (60-x) B_2O_3+20BaO+10Al_2O_3+10ZnO + xNd_2O_3(x = 0.0, 0.5, 1.0, 1.5, 2.0 and 2.5 mol%) were prepared by a conventional melt-quenching technique and studied their physical, structural, optical and luminescence properties. The amorphous nature of the glasses has been confirmed by X-ray diffraction patterns. The EDAX data shows percent mass of elements of the glass system. FTIR spectra confirm the formation of BO_3 and BO_4 groups in the glass structure and compared them with Raman spectra. The Judd-Ofelt theory was adopted to analyze the radiative properties of Nd_2O_3 –doped glasses to derive oscillator strengths (*f*), JO parameters ($\Omega_{\lambda=2,4,6}$), stimulated emission cross-sections (σ_e), radiative transition probabilities (A_R), and branching ratios (β_R) of various transitions of Nd^{3+} ions. The lifetime of the $^4F_{3/2}$ level of Nd^{3+} ions in the glasses decreases with the increase of Nd_2O_3 concentration due to the shortened distance between Nd^{3+} ion in the glass structure. The strongest emission intensity is found at 1056 nm ($^4F_{3/2} \rightarrow {}^4I_{11/2}$ transition) when excited by 808 nm. The optimum concentration of Nd_2O_3 in the studied glasses is found to be 1.0 mol% based on luminescence intensity. All these results were compared with reported research of Nd^{3+}:glasses to determine the lasing potentiality of studied glasses.

1. Introduction

Nowadays, trivalent rare-earth ion (RE^{3+}) doped materials have been more attractive due to their application in many fields such as medical, industry, electronics, and communications [1–5]. In particular, RE^{3+} ion - doped glasses become more attractive, due to their low production cost and simple preparation technique, for scintillation, optical amplification, solid-state laser applications, and microwave absorbing materials [6–8]. Among oxide glasses, borate glass is the interesting host matrix due to the high transparency, low melting point, high thermal stability, efficient radiative transition, great RE^{3+} ion solubility and homogeneity [9–12]. However, the phonon energy of borate glasses is very high around 1400 cm^{-1} that is higher than 1100, 1200, 900, 700, 500, and 350 cm^{-1} for silicate, phosphate, germanate, tellurite, fluorozirconate, and chalcogenide, respectively [13]. Hence, the present investigation is aimed to study the influence of glass composition or high energy phonons on luminescence properties of Nd^{3+} ions.

Among RE^{3+} ions, trivalent Neodymium (Nd^{3+}) ion is interesting ion for near-infrared laser application due to the strong emission at 1.06 μm

* Corresponding author. Department of Physics, Faculty of Mathematics and Natural Sciences, Institut Teknologi Bandung, Bandung - 40132, Indonesia.
** Corresponding author.
E-mail addresses: mitra@fi.itb.ac.id, mitra.djamal@yahoo.co.id (M. Djamal), suchart.kothan@cmu.ac.th (S. Kothan).

https://doi.org/10.1016/j.optmat.2020.110018
Received 21 September 2019; Received in revised form 12 May 2020; Accepted 13 May 2020

arising from $^4F_{3/2}$ to $^4I_{11/2}$ transition. The addition of Nd_2O_3 content with slight concentration will make the ion as the dopant. Meanwhile, the addition of Nd_2O_3 content with high concentration will act the ion as a modifier. However, the addition of high Nd^{3+} ion concentration can lead the concentration quenching that will reduce the fluorescence [9]. When the active ion is added to borate glass there are two possibilities. They are the conversion of BO_3 units into BO_4 units or the presence of non-bridging oxygen (NBOs) [14]. The behaviour of active ion in a host matrix depends on the surrounding ligand, which affects the emission peaks. The emission peaks of Nd^{3+} ion doped glass is originated from $^4F_{3/2}$ state. The physical, structural, optical, luminescence and non-linear optics of Nd^{3+} ion in borate aluminium glass, germanate glass, and phosphate glass were investigated [15–17]. The results show that the emission of glasses is found to be more intense in the infrared region at about 1060 nm under 808 nm excitation with high emission cross-section and long fluorescence lifetime. Therefore, it is needed to find the proper composition for borate glass with suitable modifiers to optimize the spectroscopic and luminescence properties of RE^{3+} ions.

The compound ZnO is intensively used in optoelectronic, optical, scintillating and catalytic applications due to their great functionality and physiochemical properties such as optical, thermal, photocatalytic, bioactive, and electrical [18]. The introducing ZnO in the glasses can decrease the phonon energy and improve transparency [19] of the glass. Moreover, the addition of Al_2O_3 in the glass system increase density, refractive index, improve chemical stability, physical and laser properties [20]. G. Benoit et al. reported that the addition of Al_2O_3 in the phosphate glass increase the emission intensity of active ion [21]. The alkaline earth addition such as BaO into glass improves the transition temperatures, thermal stability and create larger spectral bandwidth [22].

The present investigation is aimed to study physical, structural, optical and luminescence properties of Nd^{3+} ions in ZnO-Al_2O_3-BaO borate glasses. The experimental section describes glass preparation by melt quenching technique besides characterization techniques employed. The result and discussion section describe the amorphous nature of the present glasses, structural modifications in the glasses on doping of Nd_2O_3 through Fourier transform infrared and Raman spectroscopy. Moreover, optical band gap energies (direct and indirect) of the glasses have been evaluated from their absorption spectra. Radiative properties such as stimulated emission cross-sections (σ), radiative transition probabilities (A_R), and branching ratios (β_R) for various transitions of Nd^{3+} ions in the glasses as a function of Nd_2O_3 concentration was determined. The experimental lifetime of $^4F_{3/2}$ level was determined from its luminescent decay curve. The important conclusion drawn based on observed results are summarised in the conclusion section.

2. Experimental details

2.1. Glass composition and preparation

Zn-Al-Ba borate glasses have been fabricated by conventional melt-quenching technique. The glass composition is (60-x) B_2O_3+20BaO+10Al_2O_3+10ZnO + xNd_2O_3 where x is 0.0, 0.5, 1.0, 1.5, 2.0 and 2.5 mol%. The glasses are labeled as BBaAZNd0.0, BBaAZNd0.5, BBaAZNd1.0, BBaAZNd1.5, BBaAZNd2.0 and BBaAZNd2.5, respectively, for 0.0, 0.5, 1.0, 1.5, 2.0 and 2.5 mol% Nd_2O_3 concentrations, respectively. The raw materials have 99.99% purity and were procured from Sigma-Aldrich. They were mixed in an alumina crucible and stirred until to get homogeneity. At ambient conditions, the glass mixture was melted at 1100 °C for 3 h and mould on stainless steel plates. The bulk glass was annealed at 500 °C for 3 h to keep clear of the thermal stress. After annealing, the glass was permitted to cool off in air temperature and cut with a dimension of 1.5 × 3.0 × 0.35 cm^3. Before optical characterization, the glasses were polished to obtain a clear and transparent sample.

2.2. Characterizations

The physical properties that involve density (ρ) and molar volume (V_m) were calculated by following Archimede's principle [10,19,23]. The amorphous nature of the prepared glasses has been studied by X-ray diffractometer D8 ADVANCE from BRUKER. The Energy Dispersive Analysis of X-rays (EDAX) was adopted to know the elements present in the glasses using JEOL JSM 6510 in SEM Laboratory, FMIPA, ITB. The FTIR spectrum was recorded by Agilent Technology Cary 630 FTIR. Raman spectra of glasses were measured by Renishaw inVia Raman Microscope excited by 633 nm. Abbe refractometer (ATAGO) NAR-2T was used to measure the refractive index of glass at 589.3 nm wavelength (sodium vapour lamp) with mono-bromonaphthalene as contact liquid. The absorption spectrum in the wavelength of 400–1000 nm region was measured using Variance Cary-50 Spectrophotometer with resolution around ≤1.5 nm. The photoluminescence emission spectra and decay curves were measured by fluorescence spectrometer of Edinburgh FLS-980 where 808 nm diode laser is used as the excitation source. The resolution of Edinburgh FLS-980 spectrometer is around 1 nm. Judd-Ofelt (JO) theory is used to evaluate the spectroscopic properties of RE^{3+} ions. The area under various peaks of the absorption spectrum is used to obtain oscillator strengths (f_{cal}), JO intensity parameters ($\Omega_{\lambda=2,4,6}$), radiative transition probabilities (A_R), stimulated cross-sections (σ_R) and branching ratios (β_{cal}) [24,25]. The optical and luminescence properties have been evaluated by following the procedures described elsewhere [14,26,27].

3. Results and discussion

3.1. Physical properties

Fig. 1 presents the cut and polished glasses doped with 0.5–2.5 mol% Nd_2O_3 concentrations. The colour of the glass is darkened with the increase of Nd_2O_3 concentration in the glass system. The glass density and refractive index have been found to increase with the increase of Nd_2O_3 content. The increase of density occurs due to the higher molecular mass of Nd_2O_3 (336.48 g/mol) than B_2O_3 (69.76 g/mol).

Physical properties of BBaAZNd0.5 to BBaAZNd2.5 glass are shown in Table 1. The density and refractive index possesses a linear correlation, i.e., the denser glass sample, the higher refractive index is. Dielectric constant (e) or relative permittivity is the measurement of electrostatic flux density of material when an electric potential is applied. Dielectric constant (e) is calculated by following the procedure described elsewhere [28]. Dielectric constant (e) increase with the addition of Nd_2O_3 concentration. Dielectric constant of BBaAZNd1.0 glass is 2.41 that is lower than TAKLNP10 (3.19) [27], and ZnAlBiBNd1.0 (3.26) [29]. The low value of dielectric constant leads to huge power or frequency for loss reduction of electric power [30]. Dielectric constant is changed with change of glass composition. The derivation of dielectric constant with respect to density called optical dielectric constant expressed as P∂t/∂P. The optical dielectric constant increase with decreasing density. This corresponds to their polarizability alteration that respects to the improvement of covalent and ionic nature in the glass structure [31]. In the mole of a substance, the total polarizability can be evaluated from their refractive index and molar volume. The total polarizability corresponds to the molar polarizability (α_m) as determined [32]. Molar polarizability of glasses increases with the alteration of density (ρ) and refractive index (n) indicating the samples is more polarized due to the introducing Nd_2O_3. Nd^{3+} ion concentration in the glass system is obtained from glass density (ρ) and average molecular weight (M) [19]. Polaron radius (r_p) and inter nucleus distance (r_i) of glasses can be calculated by following the procedure described elsewhere [19,33,34]. They decrease with increase of Nd_2O_3 content as presented in Table 1.

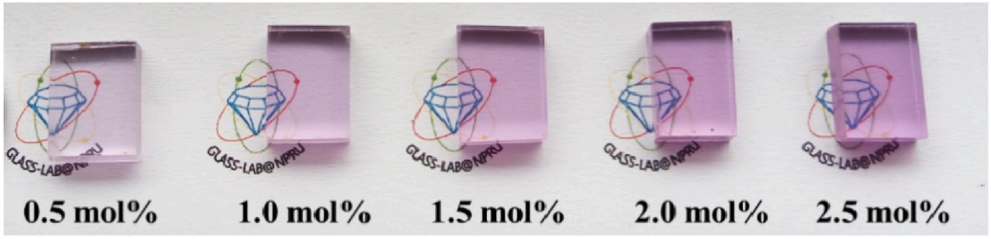

Fig. 1. Cut and polished glasses doped with 0.5–2.5 mol% Nd_2O_3.

Table 1
Physical properties of BBaAZNd glasses.

Physical properties	Glass Sample Nd_2O_3 (mol%)				
	0.5	1.0	1.5	2.0	2.5
Average molecular weight, M (g/mol)	76.848	78.182	79.516	80.849	82.183
Density, ρ (g/cm^3)	2.676	2.722	2.755	2.770	2.826
Thickness of the glass, d (cm)	0.347	0.365	0.407	0.363	0.360
Refractive index, n_d (589.3 nm)	1.549	1.552	1.554	1.558	1.567
Dielectric constant (e)	2.398	2.408	2.415	2.428	2.454
Optical dielectric constant ($P\partial t/\partial P$)	1.398	1.408	1.415	1.428	1.454
Molar volume, V_m (cm^3/mol)	28.716	28.718	28.865	29.192	29.077
Molar refractivity, R_m (cm^3/mol)	9.127	9.172	9.253	9.413	9.494
Refraction losses, R (%)	4.632	4.674	4.707	4.760	4.874
Molecular electronic polarizability, α_m (x10^{-23} cm^3)	0.362	0.363	0.367	0.373	0.376
Mn-ion concentration N (x10^{22} ions/cm^3)	1.049	2.097	3.130	4.126	5.178
Polaron radius, r_p (Å)	1.842	1.462	1.279	1.166	1.081
Interionic distance, r_i (Å)	4.569	3.626	3.173	2.894	2.683
Field Strength, F (x10^{17} cm^{-2})	1.681	2.668	3.484	4.190	4.874
free OH content, $N_{\bar{OH}}$ (x10^{19}, ion/cm^3)	0.044	0.097	0.105	0.100	0.226
Direct bandgap (eV)	3.398	3.418	3.420	3.426	3.436
Indirect bandgap (eV)	3.146	3.234	3.253	3.280	3.298

3.2. Structure

The X-ray diffraction patterns have been measured for BBaAZNd glasses and are shown in Fig. 2 for BBaAZNd1.0 glass. All the glasses under investigation exhibit broad and diffused XRD patterns. This clearly indicates amorphous nature of the glasses. Fig. 3 shows the Scanning Electron Micrograph (SEM) of BBaAZNd1.0 glass. The micrograph reveals that the BBaAZNd1.0 glass possesses porous structure. It clearly indicates that annealing at higher temperature is still needed for removing the porous structure of the glass [35]. Table 2 presents the energy dispersive analysis of X-rays (EDAX) of BBaAZNd1.0 glass. As can be seen from Table 2, the presence of Oxygen (O), Aluminium (Al), Zinc (Zn), Barium (Ba) and Neodymium (Nd) have been confirmed in the glass network. However, the element Boron (B) is not identified by EDAX [36]. Since when low energy of X-ray photon was used as excitation for low atomic number elements like B, the probability of Auger emission is higher than X-ray emission for low energy-lines, thus leads the weak X-ray fluorescence [37], that may overlap of element peaks and/or noise. Therefore, it is quite difficult to measure light atomic number elements like Boron by EDAX.

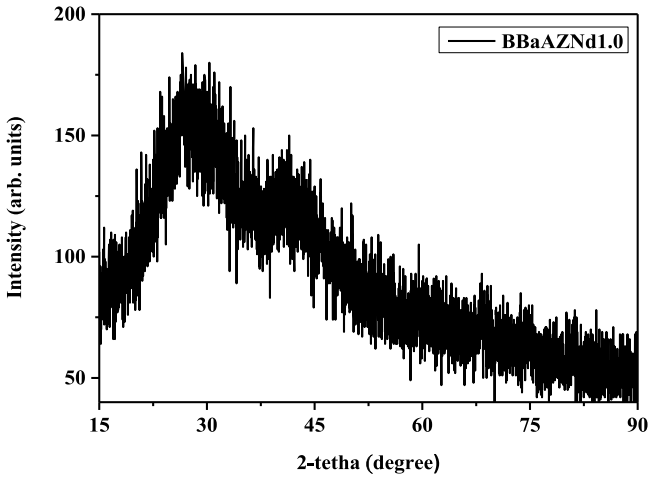

Fig. 2. X-ray diffractions of BBaAZNd1.0 glass.

FTIR and Raman spectroscopic techniques have been employed to know the vibrational modes of the functional groups present in the materials. They are complementary techniques since molecular vibrations occur through changes in the dipole moment in FTIR whereas Raman bands through polarization of molecules. There are several studies of FTIR and Raman spectra in understanding the structure of borate glasses. Fig. 4 shows the FTIR spectra of present glasses measured in 650–4000 cm^{-1} region. The vibrational bands are observed at 846-885, 945-976, 1201-1255, 1348-1380, 2920-2927 and 3259-3378 cm^{-1}. In the pure borate glass, the boroxol ring nature is confirmed by the presence of ~806 cm^{-1} absorption band. In present FTIR spectra, the boroxol ring does not observed but the BO_3 and BO_4 units in the structure of glass were confirmed. The band at 846-885 cm^{-1} arises because of the BO_4 unit symmetric stretching [38]. B-O stretching vibrations of tetragonal (BO_4) units in diborate groups are only found in the 0.5–2.5 mol% of Nd_2O_3 doped Zn-Al-Ba borate glasses centred at 945-976 cm^{-1}. Furthermore, FTIR spectra confirm B-O bond stretching of BO_4 units around 1201-1255 cm^{-1} [39]. The weak band in the 1348-1380 cm^{-1} region comes from BO_3 units asymmetric stretching and BO_2O^- [40]. The band around 2920-2927 cm^{-1} appears due to O-H band stretching vibration [41]. The band centred at 3259-3378 cm^{-1} belong to stretching vibration of OH band [41]. The FTIR spectra of BBaAZNd glass was compared with other borate glasses, namely, $30B_2O_3$ + $29TeO_2$ + 30BaO +10ZnO + $1Sm_2O_3$ (BTZOS glass) as reported [36]. The structure of BTZOS glass doesn't have much difference with BBaAZNd glass, they both have similar band and assignment including 852, 1255, 1359, 2921, and 3259 cm^{-1}. The assignments of FTIR bands of BBaAZNd glasses have been summarised in Table 3.

The free OH content ($N_{\bar{OH}}$) in the glass system can be calculated by Eq. (1) That is related to transmission in the OH band from FTIR spectra [42].

$$N_{OH^-} = \frac{N_A}{\varepsilon}\alpha_{OH^-} \quad (1)$$

Where the absorption coefficient ($\alpha_{\bar{OH}}$) at OH band (~3300 cm^{-1}) is defined by $[ln(T_O/T_D)]/L$. N_A is Avogadro's number, ε is molar absorbtivity of silicate glass 49.1 × 10^3 cm^2/mol as reported [43], T_O is maximum transmittance, T_D is transmittance at OH band (~3300 cm^{-1}), and L is glass thickness. The free OH content in the glass system has a tendency to increase by the addition of Nd_2O_3 as predicted [44]. It

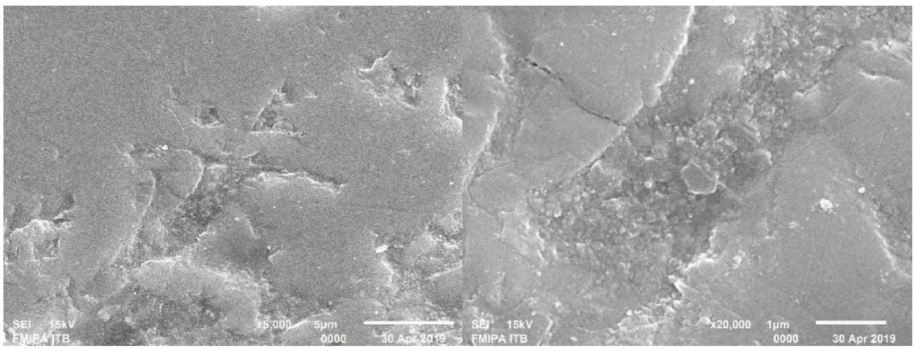

Fig. 3. Scanning electron micrograph of BBaAZNd1.0 glass.

Table 2
The energy dispersive analysis of X-rays (EDAX) of BBaAZNd1.0 glass.

Element	Energy (keV)	Relative Mass%
O	0.525	45.90
Al	1.486	14.68
Zn	8.630	11.75
Ba	4.464	23.25
Nd	5.227	4.42

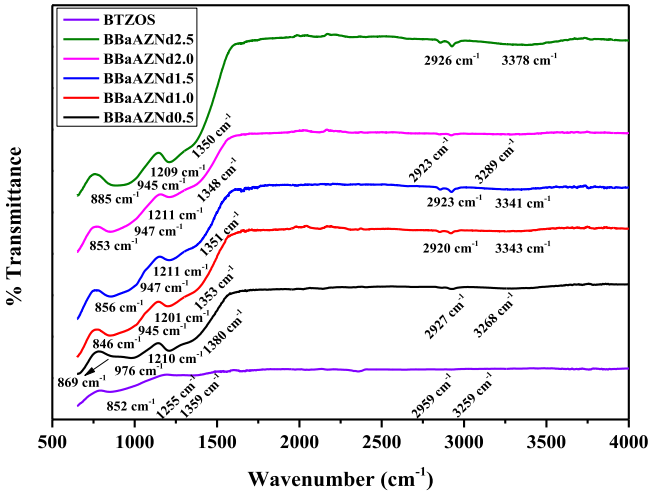

Fig. 4. FTIR spectra of BBaAZNd glasses.

indicates that Nd^{3+} ion is coupled with free OH content due to higher electronegativity of Nd^{3+} than free OH content [45]. The free OH content is found in the high temperature during melting process and can react with Nd_2O_3 to form $Nd(OH)_3$ as per following reaction possibility, namely, $Nd_2O_3 \xrightarrow{3H_2O} 2Nd(OH)_3$ [46].

Fig. 5(a) shows the Raman spectra of BBaAZNd glasses and measured between 400 and 1550 cm^{-1}. For BBaAZNd0.0 glass, the band of 459 cm^{-1} rises due to bending mode of the boroxol ring. With introduction of Nd_2O_3 into the glass structure, the peak shifts to 498 cm^{-1} and becomes wider and stronger in BBaAZNd1.0 glass compared to the other glasses due to the dominance of the bending mode of BO_4 groups and/or belongs to the movement of boron and oxygen atoms of boroxol ring in-phase [47]. The peak around 649 to 665 cm^{-1} assigns to metaborate unit [48] whereas the peak of 758–777 cm^{-1} indicates the emergence of six-membered borate rings containing one BO_4 [49] and B–O–B bending vibrations [50]. The intensity of this peak decrease while the peak of 795–800 increase with Nd_2O_3 addition in the glass network. That confirms the conversion of borate ring to boroxol ring because of the transformation of threefold to fourfold coordinated [51]. The intense vibrational mode of glasses at 904 to 968 cm^{-1} show the stretching of orthoborate unit [49]. In BBaAZNd0.0 and BBaAZNd2.5 glass, 968 cm^{-1} peak exhibit stronger than other peaks indicating the enhanced stretching of orthoborate units in the glass structure. This peak has been deconvoluted for the BBaAZNd0.0 and BBaAZNd2.5 glass samples (See Fig. 5(b)). The deconvoluted vibrational peak at about 945 cm^{-1} in BBaAZNd0.0 and BBaAZNd2.5 glasses is characteristic of an orthoborate-type structure containing BO_3 units, which can be transformed by the linking of pentaborate and tetraborate groups. The presence of orthoborate groups and the absence of pentaborate groups prove the feasibility of the transformation of pentaborate to orthoborate groups as a result of addition of Nd_2O_3 into the structure hence the structure expands. This suggests that the addition of Nd_2O_3 transformed high polymer borate units like pentaborate into low polymer groups such as boroxol rings, triborate and orthoborate groups shown in Fig. 6. The bands observed at about 1020 cm^{-1} in the spectra indicate the presence of diborate groups in these borate glasses. The number of diborate groups show less with increasing Nd_2O_3 content, as indicated by the intensity and shift observed as shown in Fig. 5(b).

$$B\emptyset_4^- \leftrightarrow B\emptyset_2O^- \quad (2)$$

Where Ø is bridging oxygen and O is non-bridging oxygen, Nd_2O_3 acts as modifier content, this fraction decreases, $B\emptyset_4^-$ units being replaced by

Table 3
The assignments of FTIR bands of BBaAZNd and BTZOS glass.

Wavenumber (cm^{-1})						Assigments	Reference
BTZOS	BBaAZNd						
	0.5	1.0	1.5	2.0	2.5		
852	869	846	856	853	885	The symmetric stretching of BO_4 unit	[38]
–	976	945	947	947	945	B-O stretching vibrations of tetragonal (BO_4) units in diborate groups	[39]
1255	1210	1201	1211	1211	1209	Stretching mode of B-O bond from BO_4 units	[39]
1359	1380	1353	1351	1348	1350	Asymmetric stretching modes of $BO_3$and BO_2O^-unit	[40]
2921	2927	2920	2923	2923	2926	Stretching vibration modes of O-H band	[41]
3259	3268	3343	3341	3289	3378	Stretching vibration modes of O-H band	[41]

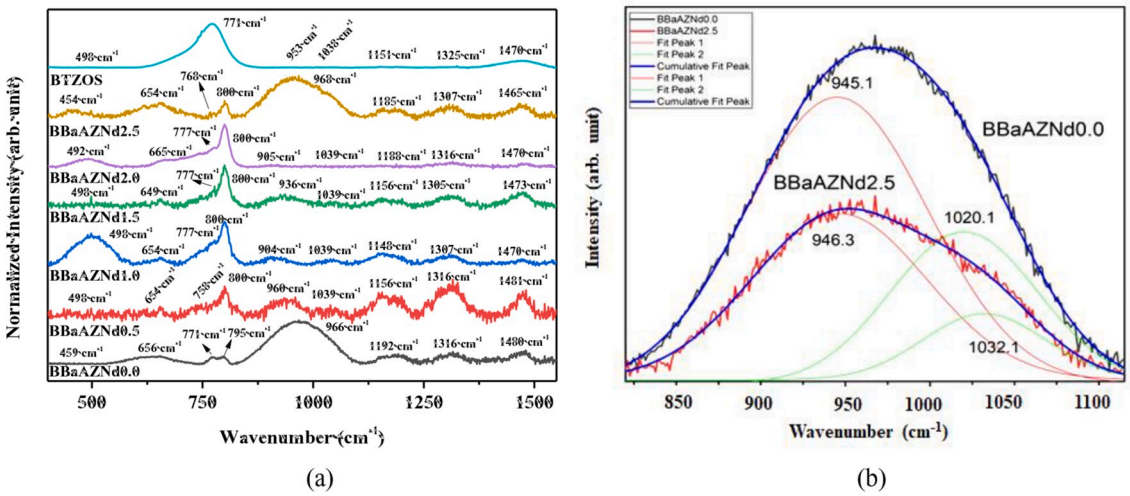

Fig. 5. (a) Raman spectra of BBaAZNd glasses, and (b) Deconvoluted graph for the BBaAZNd0.0 and BBaAZNd2.5 glasses in the range of 820–1115 cm^{-1}.

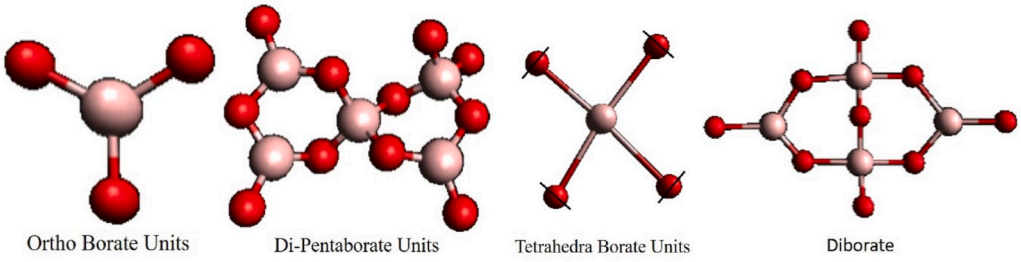

Fig. 6. Structural units of Borate groups.

boron-oxygen triangles with non-bridging oxygen atoms hence we can notice from Table .1 that the molar volume of the glasses increases with increase in Nd_2O_3 concentration. The number of non-bridging oxygens is found to be increased with increase in Nd_2O_3 content. Equation (2) shown holds good for these glasses as the tetrahedral borate groups ($B\emptyset_4^-$) are converted to triangular borate ($B\emptyset_2O^-$) network series, such as trigonal vibrations. The weak peak around 1039 show the diborate group [52]. This may also explains the stretching vibration of carbonate species (CO_3^{2-}) from ~1039 cm^{-1} due to the high basicity of borate glass [48]. The band at 1148-1192 cm^{-1} also confirms the diborate grup formation in the glass structure [49]. The band at 1305-1325 cm^{-1} verifies stretching vibrations of the BO_3 triangles in metaborate, pyroborate and ortho-borate units and these groups contain a large number of non-bridging oxygens [53]. The band at 1465-1481 cm^{-1} rise due to BO_2O- triangles linked with other borate triangular units [54]. For BBaAZNd1.0 glass, the largest phonon energy only extends to 1470 cm^{-1} which is lower than the host matrix glass (1480 cm^{-1}). The Raman spectra of BTZOS and BBaAZNd glass have been compared to understand the glass structure modification with the addition of Nd_2O_3 content. As can be seen from Fig. 5(a), for BTZOS glass, the most significant difference is the dominant appearance of 771 cm^{-1} that is covered peak around 650 and 800 cm^{-1} while for BBaAZNd glass, peak at 800 cm^{-1} is more dominant. It indicates that the formation of six-membered borate rings containing one BO_4 and B–O–B bending vibrations is more intense for BTZOS while the boroxol rings vibration is more notable for BBaAZNd glass. The Raman spectra of glasses and their assignments are presented in Table 4.

3.3. Nephelauxetic effect and bonding parameter

The nephelauxetic effect depends on covalency and polarizabilities between the central metal ion and ligands [55,56]. The nephelauxetic ratio ($\bar{\beta}$) is related to bonding parameter (δ) by Ref. [57]:

$$\delta = \left(\frac{1-\bar{\beta}}{\bar{\beta}}\right) \times 100 \quad (3)$$

Where $\bar{\beta} = \sum_N^{\beta}$ and β is the ratio of wavenumber of transition in the complex (ν_c), for example, present glass and aqua-ion (ν_a) [58] and presented in Table 5. The average of the nephelauxetic ratio ($\bar{\beta}$) of BBaAZNd1.0 glass is 0.99. The value of bonding parameter (δ) depends on whether covalent or ionic bonding of Nd^{3+} ion with their neighbouring ligands. The value of δ may be either a positive or negative. The bonding parameter (δ) of BBaAZNd1.0 glass is +0.07. The positive sign of bonding parameter shows that the BBaAZNd1.0 glass possesses higher covalency bond [59].

3.4. Optical properties: absorption spectra and bandgap energy

Fig. 7 presents the optical absorption spectra of the studied glasses. The optical absorption spectra consist of several transitions that are originated from $^4I_{9/2}$ level to various excited level including (^2P,$^2D)_{3/2}$, $^2G_{9/2}$+$^2D_{3/2}$+$^2K_{15/2}$,$^4G_{7/2}$+$^4G_{9/2}$, $^4G_{5/2}$+$^2G_{7/2}$, $^2H_{11/2}$, $^4F_{9/2}$, $^4F_{7/2}$+$^4S_{3/2}$, $^4F_{5/2}$+$^2H_{9/2}$, and $^4F_{3/2}$ states, which are peaked at 428, 475, 524,581, 625, 678, 739, 800, and 872 nm, respectively. The spectral shapes and positions of these transitions are similar to reported ones [60,61]. As can be seen from Fig. 7, the strongest transition called hypersensitive transition is centred at 581 nm due to transition from $^4I_{9/2}$ level to $^4G_{5/2}$+$^2G_{7/2}$ level. The hypersensitive transition follows the quadrupole selection rules, i.e. $\Delta J \leq 2$; $\Delta L \leq 2$; $\Delta S \leq 0$ [62,63].

The bandgap energy is an important parameter to study the electronic structure of amorphous material. Absorption coefficient α(v) corresponds to the optical bandgap following Mott and Davis relation

Table 4
Raman modes of BBaAZNd glasses and their assignments.

Wavenumber (cm^{-1})							Assigment
BTZOS	BBaAZNd						
	0.0	0.5	1.0	1.5	2.0	2.5	
498	459	498	498	498	492	444	Bending mode of BO_4 groups and/or movement of boron and oxygen atom of boroxol ring in-phase [47]
-	656	654	654	649	665	654	Metaborate unit [48]
771	771	758	777	777	777	768	Six-membered borate rings containing one BO_4 [49], B–O–B bending vibrations [50]
-	795	800	800	800	800	800	Vibration of boroxol rings [51]
953	966	960	904	936	905	968	Stretching of orthoborate unit [49]
1038	-	1039	1039	1039	1039	-	Diborate group [52], stretching vibration of carbonate species (CO_3^{2-}) [48]
1151	1192	1156	1148	1156	1188	1185	Diborate unit [49]
1325	1316	1316	1307	1305	1316	1307	Stretching vibrations of the BO3 triangles in metaborate, pyroborate and ortho-borate units and these groups contain a large number of non-bridging oxygens [53]
1470	1480	1481	1470	1473	1470	1465	BO_2O- triangles linked t other borate triangular units [54]

[64].

$$\alpha(v) = \frac{B_0\left(hv - E_g^{opt}\right)^n}{hv} \quad (4)$$

Where B_0 is constant, E_g^{opt} is optical bandgap energy, n is half (1/2) for allowed direct transition and two (2) for the allowed indirect transition. The bandgap energy is determined by plotting the relationship between *hν* as x-axis and $(ahv)^n$ as y-axis. The extrapolation of the absorption edge of the graph is shown the optical bandgap energy as presented in Fig. 8 (direct bandgap) and Fig. 9 (indirect bandgap). The direct and indirect bandgap energies of the glasses are found to be in the range of 3.40–3.44 eV and 3.15–3.30 eV, respectively. Both direct and indirect bandgap energy of the glasses increases by the addition of Nd_2O_3 concentration as shown in Fig. 10. The increase of bandgap energy indicates the decrease of glass structure disorder [65]. The present glass band gap energy is higher than Nd^{3+} ion-doped soda lime silicate [66] and lower than lithium magnesium borate glass [10].

3.5. Photoluminescence properties

Emission spectra of BBaAZNd glasses were presented in Fig. 11(a). These glasses were excited by $\lambda_{ex} = 808$ nm and the resultant emissions in the wavelength 800 nm–1500 nm range are generated by transitions from $^4F_{3/2}$ level to $^4I_{9/2}$, $^4I_{11/2}$, and $^4I_{13/2}$ level, which are centred around 875 nm, 1056 nm, and 1327 nm, respectively [67–69]. The emission intensity is increased with the increase of Nd_2O_3 concentration from 0.5 mol% to 1.0 mol% and then decreased with further increase of Nd_2O_3 content beyond 1.0 mol%, indicating that the optimum concentration of Nd_2O_3 concentration is 1.0 mol%. Fig. 11(b) represents the

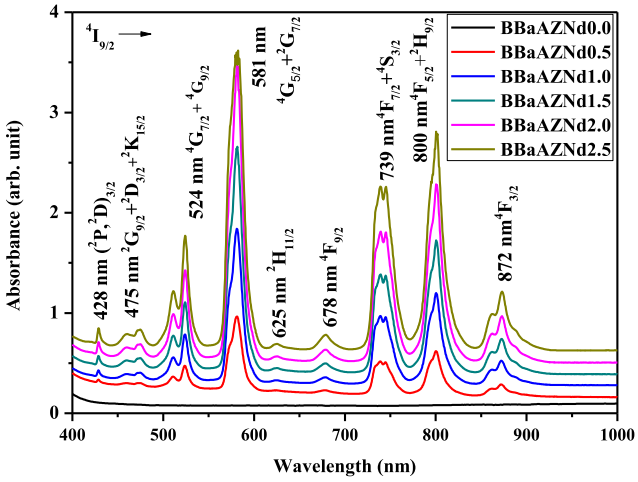

Fig. 7. Optical absorption spectra of BBaAZNd glasses.

Table 5
Transition, peak position (λ, nm), wavenumber of transition in complex (ν_c, cm^{-1}) and in aquo-ion (ν_a, cm^{-1}), experimental and calculated oscillator strength (*f*, $\times 10^{-6}$), and JO parameters (Ω_λ, $\times 10^{-20}$ cm^2) of BBaAZNd glasses.

Transition $^4I_{9/2}\rightarrow$	λ	ν_c	ν_a	BBaAZNd0.5		BBaAZNd1.0		BBaAZNd1.5		BBaAZNd2.0		BBaAZNd2.5	
				f_{exp}	f_{cal}	f_{exp}	f_{cal}	f_{exp}	f_{cal}	f_{exp}	f_{cal}	f_{exp}	f_{cal}
$(^2P,^2D)_{3/2}$	428	23364	23140	0.49	0.41	0.43	0.36	0.28	0.32	0.23	0.37	0.31	0.37
$^2G_{9/2}+^2D_{3/2}+^2K_{15/2}$	475	21053	21016	2.40	1.75	2.14	1.24	1.05	1.22	1.10	1.56	1.35	1.54
$^4G_{7/2}+^4G_{9/2}$	524	19084	19103	8.00	7.15	7.35	6.10	4.95	4.94	6.80	6.13	5.78	6.02
$^2G_{7/2}+^4G_{5/2}$	581	17212	17167	30.10	30.14	24.45	24.44	21.19	21.19	23.12	23.17	22.34	22.34
$^2H_{11/2}$	625	16000	16026	0.76	0.23	0.27	0.20	0.09	0.17	0.11	0.21	0.18	0.20
$^4F_{9/2}$	678	14749	14854	1.04	0.84	0.78	0.73	0.22	0.63	0.47	0.75	0.76	0.74
$^4F_{7/2}+^4S_{3/2}$	739	13532	13565	10.75	10.84	9.18	9.42	8.07	8.31	9.41	9.72	9.33	9.63
$^4F_{5/2}+^2H_{9/2}$	800	12500	12573	10.18	10.19	9.23	8.91	7.84	7.49	9.49	9.09	9.41	8.99
$^4F_{3/2}$	872	11468	11527	2.50	2.98	2.47	2.67	1.72	1.98	2.07	2.66	2.41	2.63
				$\Omega_2 = 7.97$		$\Omega_2 = 6.06$		$\Omega_2 = 5.80$		$\Omega_2 = 5.60$		$\Omega_2 = 5.28$	
				$\Omega_4 = 5.65$		$\Omega_4 = 5.15$		$\Omega_4 = 3.52$		$\Omega_4 = 4.99$		$\Omega_4 = 4.88$	
				$\Omega_6 = 7.66$		$\Omega_6 = 6.63$		$\Omega_6 = 5.90$		$\Omega_6 = 6.83$		$\Omega_6 = 6.72$	
				$\Omega_2>\Omega_6>\Omega_4$		$\Omega_6>\Omega_2>\Omega_4$		$\Omega_6>\Omega_2>\Omega_4$		$\Omega_6>\Omega_2>\Omega_4$		$\Omega_6>\Omega_2>\Omega_4$	
				$\Omega_4/\Omega_6 = 0.74$		$\Omega_4/\Omega_6 = 0.78$		$\Omega_4/\Omega_6 = 0.60$		$\Omega_4/\Omega_6 = 0.73$		$\Omega_4/\Omega_6 = 0.73$	
				RMS = 0.44 × 10^{-6}		RMS = 0.16 × 10^{-6}		RMS = 0.22 × 10^{-6}		RMS = 0.39 × 10^{-6}		RMS = 0.21 × 10^{-6}	

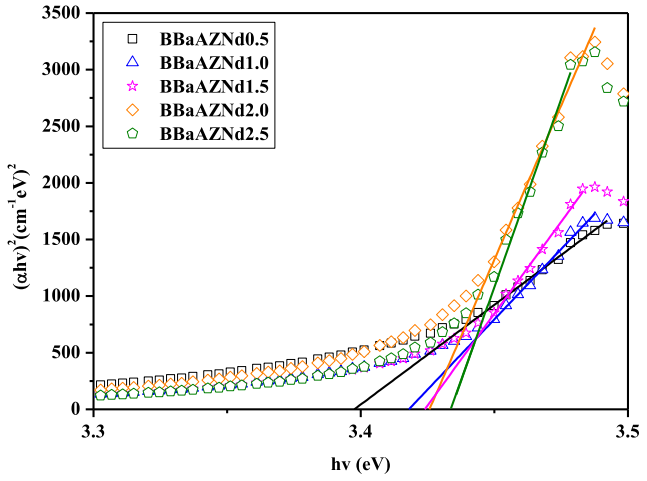

Fig. 8. Mott and Davis plots for the evaluation of the direct bandgap energies of BBaAZNd glasses.

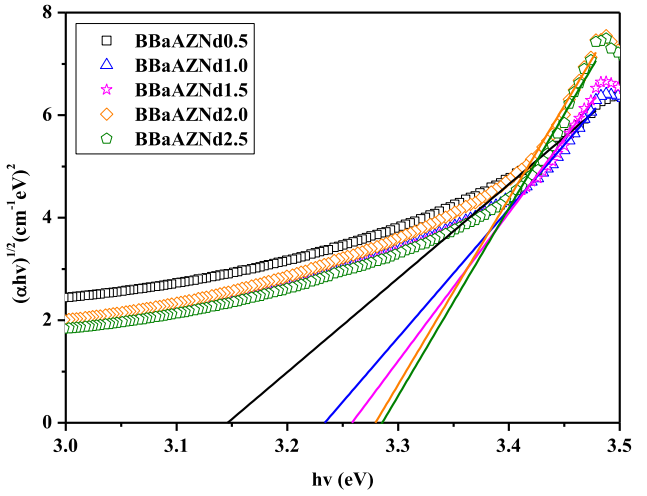

Fig. 9. Mott and Davis plots for the evaluation of the indirect bandgap energies of BBaAZNd glasses.

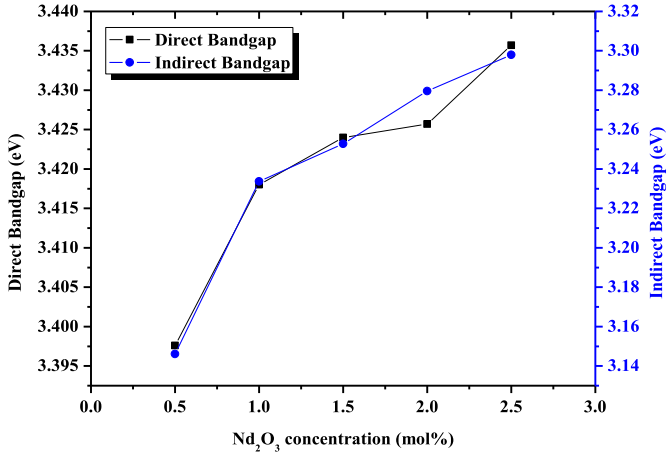

Fig. 10. The variation of direct-indirect bandgap energies of as a function of Nd_2O_3 concentration.

partial energy level diagram of Nd^{3+} ions in BBaAZ glass along with cross-relaxation channel. When Nd^{3+} ions excited by 808 nm, electrons are jumped from $^4I_{9/2}$ level to ($^4F_{5/2}$, $^2H_{9/2}$) level. The transition from this excited ($^4F_{5/2}$, $^2H_{9/2}$) state to metastable $^4F_{3/2}$ state is non-radiative due to multi-phonon relaxation. So that the transition does not generate photons but produced phonons. Radiative transitions are produced by electrons movement from $^4F_{3/2}$ level to $^4I_{9/2}$, $^4I_{11/2}$, and $^4I_{13/2}$ level. From Fig. 11(b), it can be concluded that 808 nm wavelength is suitable wavelength to pump and populate electrons in metastable state $^4F_{3/2}$.

3.6. Judd-Ofelt analysis

Experimental oscillator strengths and calculated oscillator strengths ($f \times 10^{-6}$) of various transitions of Nd^{3+} ion in the host glass matrix are shown in Table 5. Oscillator strengths of various transitions indicate how strong the absorbance is [70]. The JO parameters (Ω_λ) are derived by a least-square fitting approximation and obtained the best fit between calculated (f_{cal}) and experimental (f_{exp}) oscillator strength, with RMS value 0.16–0.44 $\times 10^{-6}$ for all present glasses. The JO parameters value depend on the glass composition and determine the local structure of the ligand field neighbouring the Nd^{3+} ion. The JO parameter trend line for BBaAZNd0.5 glass has been found to be $\Omega_2>\Omega_6>\Omega_4$ whereas for the remaining glasses it is found to be $\Omega_6>\Omega_2>\Omega_4$. The JO parameter Ω_2 indicates the covalent bond strength between Nd^{3+} ion and surrounding ligands. The greater Ω_2, the stronger covalent bond and affect the local structure of the glass towards more asymmetric. The value of Ω_2 parameter decreases on increasing Nd_2O_3 concentration indicating the reduction of covalent bond nature (See Table 5). Moreover, the reduction of Ω_2 value is followed by the increase of optical bandgap. The JO parameter (Ω_λ), JO trend line and spectroscopic quality factor (χ) of glasses and other reported Nd^{3+}:glasses are listed in Table 7. On the other hand, viscosity and rigidity of the glass are correlated to Ω_4 and Ω_6 parameters. According to R.R Jacobs and J. Weber [71], the emission intensity of the $^4F_{3/2} \rightarrow {}^4I_{11/2}$ transition of Nd^{3+} is characterized by the ratio of Ω_4 and Ω_6 parameters since Ω_2 does not contribute in determining the intensity as $||U^2||^2$ is zero for these transition. The ratio is called spectroscopic quality factor (χ). The χ value is found to be 0.74, 0.78, 0.60, 0.73, and 0.73 for BBaAZNd0.5, BBaAZNd1.0, BBaAZNd1.5, BBaAZNd2.0, and BBaAZNd2.5 glass, respectively. The smaller the ratio, the more the intensity of the $^4F_{3/2} \rightarrow {}^4I_{11/2}$ transition is. The maximum intensity of $^4F_{3/2} \rightarrow {}^4I_{11/2}$ emission can be achieved when $\Omega_6 \gg \Omega_4$ [71, 72]. The smaller spectroscopy quality factor (χ), the higher 1056 nm emission [23]. As can be clearly seen from Fig. 11 (a), the intensity (corresponding χ values) of the $^4F_{3/2} \rightarrow {}^4I_{11/2}$ laser transition for the studied glasses is found to be in the order of BBaAZNd0.5 (0.74) < BBaAZNd2.5 (0.73) <. BBaAZNd2.0 (0.73) < BBaAZNd1.5 (0.60) < BBaAZNd1.0 (0.78). Therefore, based on χ values, intensity of the BBaAZNd1.5 glass is supposed to have strongest emission as it exhibits lowest χ value compared to BBaAZNd1.0 glass and other glasses in the present investigation. But experimentally, it is observed that intensity of the BBaAZNd1.0 glass exhibit strongest emission compared to BBaAZNd1.5 glass and other glasses in the present investigation (see Fig. 11). This might be due to structural variations of BBaAZNd1.0 glass at 498 cm^{-1} (see Fig. 5(a)) compared to other glasses. The peak at 498 cm^{-1} (498 cm^{-1}) is broad and intense compared to other peaks for BBaAZNd1.0 glass i.e., high intensity vibrational energy corresponds to the BO_4 groups and/or movement of boron and oxygen atom of boroxol ring may be coupled electronic levels of Nd^{3+} ions. These low energy phonons may be responsible for lowering non-radiative relaxation consequently higher radiative transition probabilities leads to high luminescence intensity compared to BBaAZNd1.5 and other glasses. The χ values of the studied glasses are found to lower than TZNLN [69], BSGdCaNd0.5 [7], PKCFAN10 [33], SPbKNLFNd10 [26], NKZLSNd10 [68], TZNLNd [73], D glass [74], TZN10 [75], and SrLiBO [76] glasses. The JO parameter (Ω_λ), JO trend line and spectroscopic quality factor (χ) of glasses and other reported Nd^{3+}:glasses are listed in Table 7. The JO

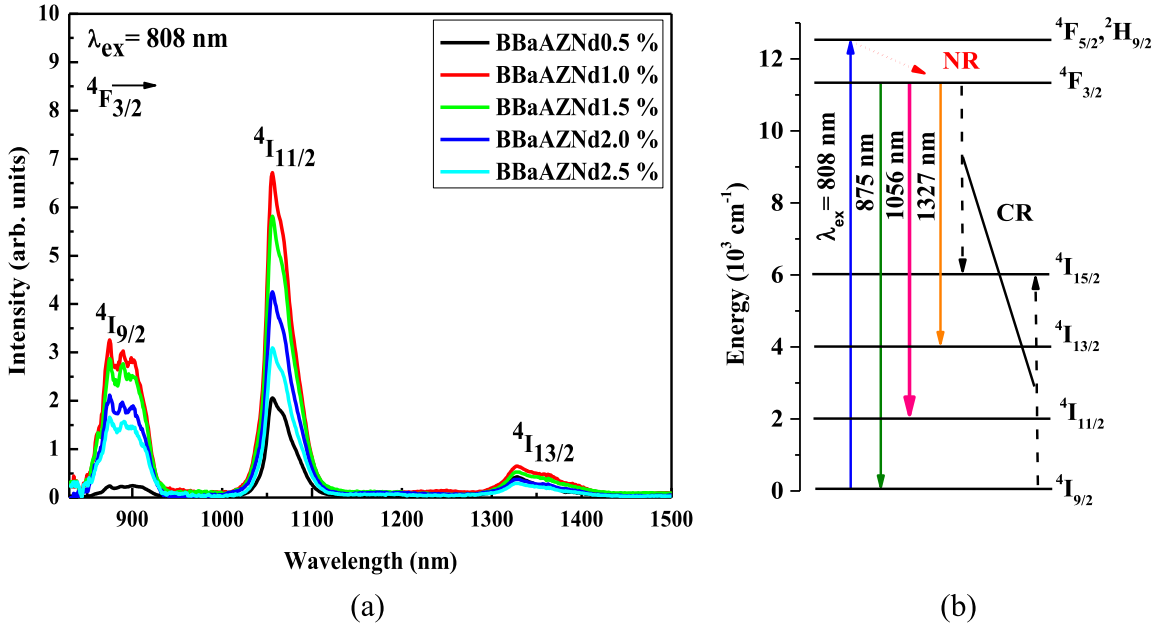

Fig. 11. (a) Photoluminescence spectra, and (b) partial energy level structure and cross-elaxation channel of Nd^{3+} ions in BBaAZ glasses.

Table 6
Wavelength (λ, nm), calculated (β_{cal}) and experimental branching ratios (β_{exp}), stimulated emission cross-section (σ_e) and radiative transition probability (A_R) for various transitions of Nd^{3+} ions in BBaAZ glasses.

Glass code	Transition $^4F_{3/2}$→	λ (nm)	β_{cal}	β_{exp}	$\sigma_e \times 10^{-20}$ cm^2	A_R (s^{-1})
BBaAZNd0.5	$^4I_{9/2}$	875	0.38	0.10	1.04	1567
	$^4I_{11/2}$	1056	0.51	0.68	3.74	2092
	$^4I_{13/2}$	1327	0.11	0.22	1.20	433
	A_T (s^{-1}) = 4092					
BBaAZNd1.0	$^4I_{9/2}$	875	0.39	0.37	0.79	1419
	$^4I_{11/2}$	1056	0.51	0.54	3.03	1842
	$^4I_{13/2}$	1327	0.10	0.09	0.81	377
	A_T (s^{-1}) = 3638					
BBaAZNd1.5	$^4I_{9/2}$	875	0.35	0.36	0.65	1047
	$^4I_{11/2}$	1056	0.53	0.55	2.80	1566
	$^4I_{13/2}$	1327	0.11	0.09	0.77	337
	A_T (s^{-1}) = 2950					
BBaAZNd2.0	$^4I_{9/2}$	875	0.38	0.36	0.76	1414
	$^4I_{11/2}$	1056	0.51	0.55	2.96	1898
	$^4I_{13/2}$	1327	0.11	0.09	0.79	393
	A_T (s^{-1}) = 3705					
BBaAZNd2.5	$^4I_{9/2}$	875	0.38	0.36	0.82	1411
	$^4I_{11/2}$	1056	0.52	0.55	3.30	1899
	$^4I_{13/2}$	1327	0.11	0.09	0.92	394
	A_T (s^{-1}) = 3704					

trendline of BBaAZNd1.0 glass is $\Omega_6 > \Omega_2 > \Omega_4$ indicating higher rigidity in the glass structure.

Table 6 shows branching ratios (β_{cal}), stimulated emission cross-sections (σ_e), and radiative transition probabilities (A_R) of BBaAZNd glasses for all transition of emission spectra. The branching ratios (β_{cal}) and radiative transition probabilities (A_R) have been calculated by employing JO theory to absorption spectra. Total radiative transition probability (A_T) is associated with radiative lifetimes (τ_{rad}) [45,61,77]. The greater A_T, the faster decay time occurs. The total radiative transition probability (A_T) of BBaAZNd1.0 glass in $^4F_{3/2}$ level is 3638 s^{-1} and the radiative lifetime is 275 μs. The relative intensity of the transition in the emission spectra is known as experimental branching ratio (β_{exp}), that is given by the ratio of the transition intensity and total transitions intensity in the emission spectra. The $^4F_{3/2} \rightarrow {}^4I_{11/2}$ transition of BBaAZNd1.0 glass centred at 1056 nm has radiative transition probability $A_R = 1842\ s^{-1}$, experimental branching ratios $\beta_{exp} = 0.54$ and stimulated emission cross-section $\sigma_e = 3.03 \times 10^{-20}$ cm^2. The standard deviation value (δ_{stdv}) of A_R, β_{exp}, and σ_e is ±5.25, ±0.007, and ±0.11 × 10^{-21}, respectively. Branching ratios (β_R) is an important parameter to describe a laser gain medium. The branching ratios for laser gain medium should be $\beta \geq 0.5$ for high lasing power [78].

Table 7 shows the comparison of stimulated emission cross-section (σ_e), effective bandwidth ($\Delta\lambda_{eff}$), and gain bandwidth ($\sigma_e \times \Delta\lambda_{eff}$) of BBaAZNd glasses at 1056 nm with reported Nd^{3+}:glasses. The glass medium should have high stimulated emission cross-section (σ_e) value for a laser application [79]. From Table 7, the stimulated emission cross-section of BBaAZNd1.0 glass at 1056 nm is greater than PKMFAN10 [80], BSGdCaNd0.5 [7] and TAKLNP10 [27]. The gain bandwidth is the frequency range where optical amplification will be achieved. The gain bandwidth of BBaAZNd0.5 glass is 1.26 × 10^{-25} cm^3. This value is higher than PKMFAN10 [80], BSGdCaNd0.5 [7], SPbKNLFNd10 [26], TAKLNP10 [27], PKFBAN10 [81] and TZNLNd [73]. Due to the high gain bandwidth, BBaAZNd0.5 glass possesses high potential for a broadband optical amplification [26]. However, for further laser application, the advance experiment could be needed to observe the glass sample directly in the laser system, as none of the present glass in Table 7 was tried in the laser experiment.

3.7. Lifetimes

Luminescent decay curves for the determination of experiment lifetimes for the $^4F_{3/2}$ level of Nd^{3+} ions in BBaAZNd glasses are presented in Fig. 12. The decay curves have been observed by recording 1056 nm emission under 808 nm excitation. It is found that luminescence decay of all glasses is bi-exponential and the average lifetime of glasses for $^4F_{3/2} \rightarrow {}^4I_{11/2}$ is measured by Eq. (5).

$$\tau_{ave} = \frac{A_1\tau_1^2 + A_2\tau_2^2}{A_1\tau_1 + A_2\tau_2} \quad (5)$$

Where τ_{ave} shows the experimental lifetime (τ_{exp}); A_1 and A_2 are constant; τ_1 and τ_2 are short and long decay time. The experimental lifetime (τ_{exp}) is found to be 58, 52, 46, 40, and 32 μs for BBaAZND0.5, BBaAZNd1.0, BBaAZNd1.5, BBaAZNd2.0, and BBaAZNd2.5, respectively. Therefore, the experimental lifetime (τ_{exp}) is decreased with increasing Nd_2O_3 concentration due to energy transfer between Nd^{3+}

Table 7
JO parameters ($\Omega_\lambda \times 10^{-20}$ cm^2), and their trendline, χ (Ω_4/Ω_6), stimulated emission cross-section ($\sigma_e \times 10^{-20}$ cm^2), effective bandwidth ($\Delta\lambda_{eff}$, nm), and gain bandwidth ($\sigma_e \times \Delta\lambda_{eff}$, $\times 10^{-25}$ cm^3) at 1056 nm emission of BBaAZNd glasses along with reported Nd^{3+}:glasses.

Glass Code	Ω_2	Ω_4	Ω_6	Trendline	X	σ_e	$\Delta\lambda_{eff}$	$\sigma_e x \Delta\lambda_{eff}$
BBaAZNd0.5 [p.w]	7.97	5.65	7.66	$\Omega_2>\Omega_6>\Omega_4$	0.74	3.74	33.78	1.26
BBaAZNd1.0 [p.w]	6.06	5.15	6.63	$\Omega_6>\Omega_2>\Omega_4$	0.78	3.03	36.75	1.11
BBaAZNd1.5 [p.w]	5.80	3.52	5.90	$\Omega_6>\Omega_2>\Omega_4$	0.60	2.80	33.88	0.95
BBaAZNd2.0 [p.w]	5.60	4.99	6.83	$\Omega_6>\Omega_2>\Omega_4$	0.73	2.96	38.72	1.15
BBaAZNd2.5 [p.w]	5.28	4.88	6.72	$\Omega_6>\Omega_2>\Omega_4$	0.73	3.30	34.79	1.15
TZNLN [69]	2.13	3.29	3.83	$\Omega_2<\Omega_4<\Omega_6$	0.86	4.27	28.35	1.21
PKCFAN10 [33]	5.40	7.03	6.51	$\Omega_2<\Omega_6<\Omega_4$	1.08	3.42	–	–
PKMFAN10 [80]	4.41	2.88	4.06	$\Omega_4<\Omega_6<\Omega_2$	0.70	1.81	40.40	0.73
BSGdCaNd0.5 [7]	2.14	2.57	1.93	$\Omega_6<\Omega_2<\Omega_4$	1.33	1.39	32.90	0.46
SPbKNLFNd10 [26]	6.89	10.09	9.09	$\Omega_2<\Omega_6<\Omega_4$	1.10	4.11	36.40	0.01
NKZLSNd10 [68]	10.26	6.38	6.06	$\Omega_2>\Omega_4>\Omega_6$	1.05	4.30	38.00	1.63
TAKLNP10 [27]	5.93	3.23	4.69	$\Omega_4<\Omega_6<\Omega_2$	0.67	3.00	35.00	1.05
PKFBAN10 [81]	4.92	3.67	5.26	$\Omega_4<\Omega_2<\Omega_6$	0.70	3.67	27.97	1.03
TZNLNd [73]	3.91	2.65	2.92	$\Omega_6>\Omega_4>\Omega_2$	0.91	3.69	25.88	0.96
D glass [74]	3.22	3.84	4.33	$\Omega_6>\Omega_4>\Omega_2$	0.89	3.80	30.60	1.16
TZN10 [75]	3.80	4.94	4.54	$\Omega_4<\Omega_6<\Omega_2$	1.09	4.27	30.90	1.32
SrLiBO [76]	6.52	5.00	6.16	$\Omega_2<\Omega_6<\Omega_4$	0.81	–	–	–

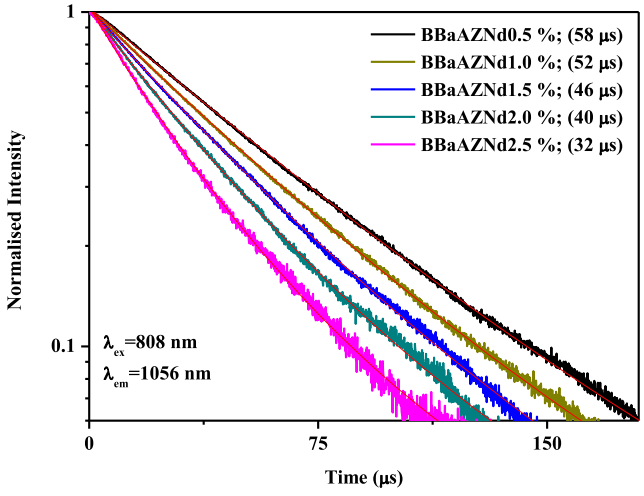

Fig. 12. Luminescence decay curves for $^4F_{3/2}$ level of BBaAZNd glasses fitted by bi-exponential.

ions and/or Nd^{3+}ions and host defects in the glass structure. The energy transfer takes place between the excited Nd^{3+} ions and ground state Nd^{3+} ions through cross-relaxation $^4F_{3/2} + {}^4I_{9/2} \rightarrow {}^4I_{15/2} + {}^4I_{15/2}$, which is responsible for decrease of lifetimes of $^4F_{3/2}$ level of Nd^{3+} ions in the studied glasses. The radiative lifetime (τ_{rad}) of all glasses is found to be higher than experimental lifetimes (τ_{exp}) because of the high phonon energy of borate glass. The quantum efficiency of the studied glasses is estimated by the ratio of the experiment lifetime and radiative lifetime (τ_{exp}/τ_{rad}). BBaAZNd glasses possesses the quantum efficiency in the range of 12% to 24% as presented in Table 8. The low-efficiency of BBaAZNd glasses indicates higher non-radiative transition processes in the borate glasses [82]. Previous research also reported low quantum efficiency for borate glasses [7,74].

Table 8
Experimental (τ_{exp}), radiative lifetime (τ_{rad}), efficiency (η), and non-radiative transition rate (W_{NR}) of BBaAZNd glasses.

Glass code	τ_{exp} (μs)	τ_{rad} (μs)	η (%)	W_{NR} (s^{-1})
BBaAZNd0.5	58	244	24	13149
BBaAZNd1.0	52	275	19	15593
BBaAZNd1.5	46	339	14	18789
BBaAZNd2.0	40	270	15	21295
BBaAZNd2.5	32	270	12	27546

3.8. Non-radiative process analysis

The vibration of the host matrix can lead Nd^{3+} ion in the excited state transfer their energy to the host matrix and relax to lower energy state without light emission called non-radiative transition. The non-radiative transition rate (W_{NR}) includes multiphonon relaxation rate, concentration quenching, energy transfer to luminescence quenching centres like hydroxyl (OH^-) groups etc. The non-radiative transition rate due to hydroxyl (OH^-) group is negligible, since the OH^- concentration in the present glasses is very low (see Table 1). Hence, the non-radiative transition rate (W_{NR}) can be calculated using experiment (τ_{exp}) and radiative (τ_{rad}) decay time by following Eq. (6).

$$W_{(NR)} = \frac{1}{\tau_{exp}} - \frac{1}{\tau_{rad}} \quad (6)$$

Table 8 shows the non-radiative rate of BBaAZNd glasses along with their lifetime and efficiency. With increase of Nd_2O_3 concentration the interaction between ions is very important as the distance Nd^{3+}-Nd^{3+} become closer leading to fast quenching process. Since the efficiency of glasses decreases with the addition of Nd_2O_3, the non-radiative rate of glasses increase that is affected by the glass luminescence. The high W_{NR} may occur due to energy transfer through the cross-relaxation process between Nd^{3+} ion via ($^4F_{3/2}$+$^4I_{9/2}$)→($^4I_{15/2}$+$^4I_{15/2}$) or ($^4F_{3/2}$+$^4I_{9/2}$)→($^4I_{13/2}$+$^4I_{15/2}$) channel as shown in Fig. 11(b). According to W.T. Carnall et al., the difference energy gap of $^4F_{3/2}$ and $^4I_{15/2}$ level of Nd^{3+} ion is 5447 cm^{-1}. For BBaAZNd1.0 glass, the phonon energy is around 1470 cm^{-1}, so that three to four phonons are enough to bridge the energy gap allowing multiphonon relaxation process for $^4F_{3/2}$ level.

The local crystal-field symmetry of glasses can be involved in the non-radiative transition rate by depopulating excited state level through the local vibrational mechanism. Such mechanism occurs when Nd^{3+} ion decay non-radiatively via lattice vibrational and reduce the luminescence [80]. This process is avoided for laser gain development since high quantum efficiency should be achieved. The high W_{NR} produces the increase of thermal population in emission state, the increment of multiphonon decay, and decrease of fluorescence decay time. Among glasses, the highest efficiency with lowest non-radiative transition rate is obtained by BBaAZNd0.5 glass. The high W_{NR} can be reduced by lowering the borate content accompanied by the addition of heave metal oxides such as TeO_2.

4. Conclusion

The Zn-Al-Ba borate glasses doped with Nd^{3+} ions were fabricated and studied their structural and optical properties. The addition of

Nd_2O_3 in the glasses has improved the physical properties such as increasing the density, molecular electronic polarizability, and field strength; decrease the polaron radius and interionic distance. The broad and diffused X-ray diffraction patterns confirmed the amorphous nature of the glasses. The FTIR spectrum reflects the characteristic vibration modes of BO_3 units, BO_4 units, and OH groups in the studied glasses and compared with corresponding Raman spectra. The phonon energy of 1 mol% Nd_2O_3 doped Zn-Al-Ba borate glasses is about 1470 cm^{-1}. Both direct (3.40–3.44 eV) and indirect (3.15–3.30 eV) bandgap energies are increased with the increase of Nd_2O_3 concentration. The JO parameter trendline is found $\Omega_2>\Omega_6>\Omega_4$ for BBaAZNd0.5 and $\Omega_6>\Omega_2>\Omega_4$ for the rest of glasses. The radiative properties for BBaAZNd0.5 glass at 1056 nm is found as $A_R = 2092\ s^{-1}$, $\beta_{exp} = 0.68$ and $\sigma_e = 3.74 \times 10^{-20}$ cm^2. The gain bandwidth of BBaAZNd0.5 glass for $^4F_{3/2} \rightarrow {}^4I_{11/2}$ transition has been found to be 1.26×10^{-25} cm^3. All the results indicate that BBaAZNd0.5 glass could be useful for infrared emitting device applications.

Declaration of competing interest

The authors declare that they have no known competing financial interests or personal relationships that could have appeared to influence the work reported in this paper.

CRediT authorship contribution statement

M. Djamal: Formal analysis. **L. Yuliantini:** Formal analysis. **R. Hidayat:** Formal analysis. **N. Rauf:** Formal analysis. **M. Horprathum:** Formal analysis. **R. Rajaramakrishna:** Formal analysis. **K. Boonin:** Investigation. **P. Yasaka:** Formal analysis. **J. Kaewkhao:** Investigation, Methodology. **V. Venkatramu:** Formal analysis. **S. Kothan:** Project administration.

Acknowledgements

This work has been supported by Riset ITB 2019 (No. 91I/I1.C01/PL/2019) and WCU-ITB 2019 (No. 350C/SK/I1.B02/2019). J. Kaewkhao, K. Boonin, P. Yasaka and Ms. Lia Yuliantini would like to express her sincerely thank National Research Council of Thailand (NRCT) and Nakhon Pathom Rajabhat University (NPRU) for supporting this research and National Electronics and Computer Technology Center (NECTEC), Thailand for Raman measurement. This research was partially supported by Chiang Mai University. One of the authors Venkatramu is grateful to Department of Science and Technology (DST), New Delhi for the sanction of research project (No. INT/PORTUGAL/P-04/2017) under India-Portugal bilateral scientific and technological cooperation.

Appendix A. Supplementary data

Supplementary data to this article can be found online at https://doi.org/10.1016/j.optmat.2020.110018.

References

[1] C.-W. Chan, G.C. Smith, Fibre laser joining of highly dissimilar materials: commercially pure Ti and PET hybrid joint for medical device applications, Mater. Des. 103 (2016) 278–292, https://doi.org/10.1016/j.matdes.2016.04.086.
[2] N. Pagano, G. Campana, M. Fiorini, R. Morelli, Laser transmission welding of polylactide to aluminium thin films for applications in the food-packaging industry, Optic Laser. Technol. 91 (2017) 80–84, https://doi.org/10.1016/j.optlastec.2016.12.014.
[3] C. Constantinescu, L. Rapp, A.-P. Alloncle, Investigations on laser printing of microcapacitors using poly (methyl methacrylate) dielectric thin films for organic electronics applications, Appl. Surf. Sci. 374 (2016) 90–95, https://doi.org/10.1016/j.apsusc.2015.10.015.
[4] M. Li, L. Tan, Q. Yang, J. Ma, S. Yu, Effect of partially coherent laser source on the performance of fiber-coupling DPSK receiver for optical communication, Optic Commun. 350 (2015) 135–143, https://doi.org/10.1016/j.optcom.2015.04.004.
[5] W. Widanarto, E. Ardenti, S.K. Ghoshal, C. Kurniawan, M. Effendi, W.T. Cahyanto, Significant reduction of saturation magnetization and microwave-reflection loss in barium-natural ferrite via Nd^{3+} substitution, J. Magn. Magn Mater. 456 (2018) 288–291, https://doi.org/10.1016/j.jmmm.2018.02.050.
[6] J. Kaewkhao, N. Wantana, S. Kaewjaeng, S. Kothan, H.J. Kim, Luminescence characteristics of Dy^{3+} doped Gd_2O_3-CaO-SiO_2-B_2O_3 scintillating glasses, J. Rare Earths 34 (2016) 583–589, https://doi.org/10.1016/S1002-0721(16)60065-0.
[7] C.R. Kesavulu, H.J. Kim, S.W. Lee, J. Kaewkhao, N. Wantana, E. Kaewnuam, S. Kothan, S. Kaewjaeng, Spectroscopic investigations of Nd^{3+} doped gadolinium calcium silica borate glasses for the NIR emission at 1059 nm, J. Alloys Compd. 695 (2017) 590–598, https://doi.org/10.1016/j.jallcom.2016.11.002.
[8] Y.C. Ratnakaram, S. Babu, L.K. Bharat, C. Nayak, Fluorescence characteristics of Nd^{3+} doped multicomponent fluoro-phosphate glasses for potential solid-state laser applications, J. Lumin. 175 (2016) 57–66, https://doi.org/10.1016/j.jlumin.2016.02.009.
[9] A.K. Varshneya, Fundamentals of Inorganic Glasses, Academic Press, Boston, 1994.
[10] M.H.A. Mhareb, S. Hashim, S.K. Ghoshal, Y.S.M. Alajerami, M.A. Saleh, R. S. Dawaud, N.A.B. Razak, S.A.B. Azizan, Impact of Nd^{3+} ions on physical and optical properties of Lithium Magnesium Borate glass, Opt. Mater. 37 (2014) 391–397, https://doi.org/10.1016/j.optmat.2014.06.033.
[11] K.H. Sun, M.L. Huggins, Energy additivity in oxygen-containing crystals and glasses, J. Phys. Colloid Chem. 51 (1947) 438–443.
[12] G.N. Hemantha Kumar, J.L. Rao, K. Ravindra Prasad, Y.C. Ratnakaram, Fluorescence and Judd–Ofelt analysis of Nd^{3+} doped P_2O_5–Na_2O–K_2O glass, J. Alloys Compd. 480 (2009) 208–215, https://doi.org/10.1016/j.jallcom.2009.02.033.
[13] M. Yamane, Y. Asahara, Glasses for Photonics, Cambridge University Press, 2000.
[14] A.L.F. Novais, N.O. Dantas, I. Guedes, M.V.D. Vermelho, Spectroscopic properties of highly Nd-doped lead phosphate glass, J. Alloys Compd. 648 (2015) 338–345, https://doi.org/10.1016/j.jallcom.2015.06.148.
[15] Y. Yue, C. Shao, S. Kang, F. Wang, X. Wang, D. He, W. Chen, L. Hu, EPR study of luminescence mechanism of Nd3+-doped borate aluminate glass, Ceram. Int. 45 (2019) 6566–6569, https://doi.org/10.1016/j.ceramint.2018.12.016.
[16] S.J. Huang, Y.B. Xiao, J.L. Liu, Y. Ji, L.Y. Mao, W.C. Wang, Nd3+-doped antimony germanate glass for 1.06 μm fiber lasers, J. Non-Cryst. Solids 518 (2019) 10–17, https://doi.org/10.1016/j.jnoncrysol.2019.05.008.
[17] J. Rajagukguk, R. Situmorang, Fitrilawati, M. Djamal, R. Rajaramakrishna, J. Kaewkhao, P.H. Minh, Structural, spectroscopic and optical gain of Nd^{3+} doped fluorophosphate glasses for solid state laser application, J. Lumin. 216 (2019) 116738, https://doi.org/10.1016/j.jlumin.2019.116738.
[18] M. Wang, L. Fang, M. Li, A. Li, X. Zhang, Y. Hu, Z. Liu, R. Dongol, Glass transition and crystallization of ZnO-B_2O3-SiO_2 glass doped with Y_2O_3, Ceram. Int. 45 (2019) 4351–4359, https://doi.org/10.1016/j.ceramint.2018.11.110.
[19] I. Pal, A. Agarwal, S. Sanghi, M.P. Aggarwal, S. Bhardwaj, Fluorescence and radiative properties of Nd3+ ions doped zinc bismuth silicate glasses, J. Alloys Compd. 587 (2014) 332–338, https://doi.org/10.1016/j.jallcom.2013.10.191.
[20] Y. Yue, Y. Wang, Y. Cao, S. Chen, Q. Zhou, W. Chen, L. Hu, Effect of Al_2O_3 on structure and properties of Al_2O_3-K_2O-P_2O_5 glasses, Opt. Mater. Express 8 (2018) 245, https://doi.org/10.1364/OME.8.000245.
[21] B. Glorieux, T. Salminen, J. Massera, M. Lastusaari, L. Petit, Better understanding of the role of SiO_2, P_2O_5 and Al_2O_3 on the spectroscopic properties of Yb^{3+} doped silica sol-gel glasses, J. Non-Cryst. Solids 482 (2018) 46–51, https://doi.org/10.1016/j.jnoncrysol.2017.12.021.
[22] N. Manikandan, A. Ryasnyanskiy, J. Toulouse, Thermal and optical properties of TeO_2–ZnO–BaO glasses, J. Non-Cryst. Solids 358 (2012) 947–951, https://doi.org/10.1016/j.jnoncrysol.2012.01.003.
[23] H. Fares, I. Jlassi, S. Hraiech, H. Elhouichet, M. Férid, Radiative parameters of Nd^{3+}-doped titanium and tungsten modified tellurite glasses for 1.06 μm laser materials, J. Quant. Spectrosc. Radiat. Transf. 147 (2014) 224–232, https://doi.org/10.1016/j.jqsrt.2014.05.029.
[24] B.R. Judd, Optical absorption intensities of rare-earth ions, Phys. Rev. 127 (1962) 750–761, https://doi.org/10.1103/PhysRev.127.750.
[25] G.S. Ofelt, Intensities of crystal spectra of rare-earth ions, J. Chem. Phys. 37 (1962) 511–520, https://doi.org/10.1063/1.1701366.
[26] P. Manasa, D. Ramachari, J. Kaewkhao, P. Meejitpaisan, E. Kaewnuam, A.S. Joshi, C.K. Jayasankar, Studies of radiative and mechanical properties of Nd^{3+}-doped lead fluorosilicate glasses for broadband amplification in a chirped pulse amplification based high power laser system, J. Lumin. 188 (2017) 558–566, https://doi.org/10.1016/j.jlumin.2017.04.065.
[27] K. Linganna, R. Narro-García, H. Desirena, E. De la Rosa, Ch Basavapoornima, V. Venkatramu, C.K. Jayasankar, Effect of P2O5 addition on structural and luminescence properties of Nd^{3+}-doped tellurite glasses, J. Alloys Compd. 684 (2016) 322–327, https://doi.org/10.1016/j.jallcom.2016.05.082.
[28] N.M. Ravindra, S. Auluck, V.K. Srivastava, On the penn gap in semiconductors, Phys. Status Solidi 93 (1979) K155–K160, https://doi.org/10.1002/pssb.2220930257.
[29] Sk Mahamuda, K. Swapna, A. Srinivasa Rao, M. Jayasimhadri, T. Sasikala, K. Pavani, L. Rama Moorthy, Spectroscopic properties and luminescence behavior of Nd^{3+} doped zinc alumino bismuth borate glasses, J. Phys. Chem. Solid. 74 (2013) 1308–1315, https://doi.org/10.1016/j.jpcs.2013.04.009.
[30] E.A. Campo, Electrical properties of polymeric materials, in: Selection of Polymeric Materials, Elsevier, 2008, pp. 141–173, https://doi.org/10.1016/B978-081551551-7.50006-1.
[31] J. Schroeder, Brillouin scattering and pockels coefficients in silicate glasses, J. Non-Cryst. Solids 40 (1980) 549–566, https://doi.org/10.1016/0022-3093(80)90129-5.

[32] X. Zhao, X. Wang, H. Lin, Z. Wang, Electronic polarizability and optical basicity of lanthanide oxides, Phys. B Condens. Matter 392 (2007) 132–136, https://doi.org/10.1016/j.physb.2006.11.015.

[33] K. Linganna, C.S.D. Viswanath, R. Narro-Garcia, S. Ju, W.-T. Han, C.K. Jayasankar, V. Venkatramu, Thermal and optical properties of Nd^{3+} ions in K-Ca-Al fluorophosphate glasses, J. Lumin. 166 (2015) 328–334, https://doi.org/10.1016/j.jlumin.2015.05.024.

[34] J.E. Shelby, J. Ruller, Properties and structure of lithium germanate glasses, Phys. Chem. Glasses 28 (1987) 262.

[35] H.C. Vasconcelos, A.S. Pinto, Fluorescence properties of rare-earth-doped sol-gel glasses, in: U. Chandra (Ed.), Recent Applications in Sol-Gel Synthesis, InTech, 2017, https://doi.org/10.5772/intechopen.68534.

[36] L. Yuliantini, M. Djamal, R. Hidayat, K. Boonin, P. Yasaka, E. Kaewnuam, V. Venkatramu, J. Kaewkhao, Optical and X-ray induced luminescence of Sm^{3+}-doped borotellurite and fluoroborotellurite glasses: a comparative study, J. Lumin. 213 (2019) 19–28, https://doi.org/10.1016/j.jlumin.2019.04.016.

[37] D.C. Bell, A.J. Garratt-Reed, Energy Dispersive X-Ray Analysis in the Electron Microscope, Garland Science, 2003.

[38] J. Yongzhong, G. Shiyang, J. Yan, Z. Yuan, X. Shuping, FTIR spectroscopy of magnesium tetraborate solution, Chem. Pap. 55 (2000) 162–166.

[39] B. Karthikeyan, FTIR spectral analysis on heavy metal borate glasses, Mod. Phys. Lett. B 20 (2006) 533–538, https://doi.org/10.1142/S0217984906010688.

[40] R. Ciceo-Lucacel, I. Ardelean, FT-IR and Raman study of silver lead borate-based glasses, J. Non-Cryst. Solids 353 (2007) 2020–2024, https://doi.org/10.1016/j.jnoncrysol.2007.01.066.

[41] N. Tugrul, M. Bardakci, E. Ozturk, Synthesis of hydrophobic nanostructured zinc borate from zinc carbonate, and characterization of the product, Res. Chem. Intermed. 41 (2015) 4395–4403, https://doi.org/10.1007/s11164-014-1538-4.

[42] P.R. Rani, M. Venkateswarlu, Sk Mahamuda, K. Swapna, N. Deopa, A.S. Rao, G. V. Prakash, Structural, absorption and photoluminescence studies of Sm^{3+} ions doped barium lead alumino fluoro borate glasses for optoelectronic device applications, Mater. Res. Bull. 110 (2019) 159–168, https://doi.org/10.1016/j.materresbull.2018.10.033.

[43] L. Nemec, J. Gotz, Infrared absorption of OH- in E glass, J. Am. Ceram. Soc. 53 (1970), https://doi.org/10.1111/j.1151-2916.1970.tb16007.x, 526–526.

[44] P.R. Ehrmann, K. Carlson, J.H. Campbell, C.A. Click, R.K. Brow, Neodymium fluorescence quenching by hydroxyl groups in phosphate laser glasses, J. Non-Cryst. Solids 349 (2004) 105–114, https://doi.org/10.1016/j.jnoncrysol.2004.08.216.

[45] G.V. Vázquez, H.G. Muñoz, I. Camarillo, C. Falcony, U. Caldiño, A. Lira, Spectroscopic analysis of a novel Nd^{3+}-activated barium borate glass for broadband laser amplification, Opt. Mater. 46 (2015) 97–103, https://doi.org/10.1016/j.optmat.2015.04.009.

[46] M. Nagao, H. Hamano, K. Hirata, R. Kumashiro, Y. Kuroda, Hydration process of rare-earth sesquioxides having different crystal structures, Langmuir 19 (2003) 9201–9209, https://doi.org/10.1021/la020954y.

[47] B. Prakash Dwivedi, Vibrational Dynamics of Fast Ion Conducting [FIC] Borate Glasses, Thesis, Aligarh Muslim University, 1993, https://core.ac.uk/download/pdf/144516862.pdf.

[48] E.I. Kamitsos, G.D. Chryssikos, Borate glass structure by Raman and infrared spectroscopies, J. Mol. Struct. 247 (1991) 1–16, https://doi.org/10.1016/0022-2860(91)87058-.

[49] G.D. Chryssikos, E.I. Kamitsos, W.M. Risen, A Raman investigation of cadmium borate and borogermanate glasses, J. Non-Cryst. Solids 93 (1987) 155–168, https://doi.org/10.1016/S0022-3093(87)80035-2.

[50] S. Rada, M. Culea, E. Culea, Structure of TeO_2·B_2O_3 glasses inferred from infrared spectroscopy and DFT calculations, J. Non-Cryst. Solids 354 (2008) 5491–5495, https://doi.org/10.1016/j.jnoncrysol.2008.09.009.

[51] K. Witke, Th Hübert, P. Reich, Ch Splett, Raman spectroscopic determination of boroxol and borate ring contents in lead borate glasses, J. Raman Spectrosc. 24 (1993) 407–410, https://doi.org/10.1002/jrs.1250240704.

[52] B.N. Meera, A.K. Sood, N. Chandrabhas, J. Ramakrishna, Raman study of lead borate glasses, J. Non-Cryst. Solids 126 (1990) 224–230, https://doi.org/10.1016/0022-3093(90)90823-5.

[53] K. Nanda, N. Berwal, R.S. Kundu, R. Punia, N. Kishore, Effect of doping of Nd^{3+} ions in BaO–TeO_2–B_2O_3 glasses: a vibrational and optical study, J. Mol. Struct. 1088 (2015) 147–154, https://doi.org/10.1016/j.molstruc.2015.02.021.

[54] R. Akagi, N. Ohtori, N. Umesaki, Raman spectra of K_2O–B_2O_3 glasses and melts, J. Non-Cryst. Solids 293–295 (2001) 471–476, https://doi.org/10.1016/S0022-3093(01)00752-9.

[55] F. Gao, S. Zhang, Investigation of mechanism of nephelauxetic effect, J. Phys. Chem. Solid. 58 (1997) 1991–1994, https://doi.org/10.1016/S0022-3697(96)00139-4.

[56] A. Suchocki, S.W. Biernacki, A. Kamińska, L. Arizmendi, Nephelauxetic effect in luminescence of Cr^{3+}-doped lithium niobate and garnets, J. Lumin. 102–103 (2003) 571–574, https://doi.org/10.1016/S0022-2313(02)00620-8.

[57] S.P. Sinha, H.-H. Schmidtke, The nephelauxetic effect in rare earth complexes illustrated for praseodymium (III), Mol. Phys. 10 (1965) 7–11, https://doi.org/10.1080/00268976600100021.

[58] W.T. Carnall, P.R. Fields, K. Rajnak, Electronic energy levels in the trivalent lanthanide aquo ions. I. Pr^{3+}, Nd^{3+}, Pm^{3+}, Sm^{3+}, Dy^{3+}, Ho^{3+}, Er^{3+}, and Tm^{3+}, J. Chem. Phys. 49 (1968) 4424–4442, https://doi.org/10.1063/1.1669893.

[59] Y.A. Tanko, S.K. Ghoshal, M.R. Sahar, Ligand field and Judd-Ofelt intensity parameters of samarium doped tellurite glass, J. Mol. Struct. 1117 (2016), https://doi.org/10.1016/j.molstruc.2016.03.083.

[60] C.R. Kesavulu, H.J. Kim, S.W. Lee, J. Kaewkhao, N. Wantana, E. Kaewnuam, S. Kothan, S. Kaewjaeng, Spectroscopic investigations of Nd^{3+} doped gadolinium calcium silica borate glasses for the NIR emission at 1059 nm, J. Alloys Compd. 695 (2017) 590–598, https://doi.org/10.1016/j.jallcom.2016.11.002.

[61] F. Zaman, G. Rooh, N. Srisittipokakun, S. Ruengsri, H.J. Kim, J. Kaewkhao, Luminescence behavior of Nd^{3+}-activated soda-lime-borate glasses for solid-state lasers applications, J. Non-Cryst. Solids 452 (2016) 307–311, https://doi.org/10.1016/j.jnoncrysol.2016.09.007.

[62] R. Van Deun, K. Binnemans, C. Görller-Walrand, J.L. Adam, Judd–Ofelt intensity parameters of trivalent lanthanide ions in a $NaPO_3$–BaF_2 based fluorophosphate glass, J. Alloys Compd. 283 (1999) 59–65, https://doi.org/10.1016/S0925-8388(98)00895-0.

[63] C.R. Kesavulu, H.J. Kim, S.W. Lee, J. Kaewkhao, N. Wantana, E. Kaewnuam, S. Kothan, S. Kaewjaeng, Spectroscopic investigations of Nd^{3+} doped gadolinium calcium silica borate glasses for the NIR emission at 1059 nm, J. Alloys Compd. 695 (2017) 590–598, https://doi.org/10.1016/j.jallcom.2016.11.002.

[64] E.A. Davis, N.F. Mott, Conduction in non-crystalline systems V. Conductivity, optical absorption and photoconductivity in amorphous semiconductors, Phil. Mag. 22 (1970) 903–922, https://doi.org/10.1080/14786437008221061.

[65] N.F. Mott, E.A. Davis, Electronic processes in non-crystalline materials, Krist. Tech. 7 (1972) 55–56, https://doi.org/10.1002/crat.19720070420.

[66] P. Chimalawong, J. Kaewkhao, C. Kedkaew, P. Limsuwan, Optical and electronic polarizability investigation of Nd^{3+}-doped soda-lime silicate glasses, J. Phys. Chem. Solid. 71 (2010) 965–970, https://doi.org/10.1016/j.jpcs.2010.03.044.

[67] R.Sk Nayab, T. S, A. Mohan Babu, L. Rama Moorthy, C.k. J, Optical spectroscopy, 1.06 μm emission properties of Nd^{3+}-doped phosphate based glasses, Spectrochim. Acta Mol. Biomol. Spectrosc. 180 (2017) 193–197, https://doi.org/10.1016/j.saa.2017.03.012.

[68] D. Ramachari, M. Rama, C.K. Jayasankar, Optical absorption and emission properties of Nd^{3+}-doped oxyfluorosilicate glasses for solid state lasers, Infrared Phys. Technol. 67 (2015) 555–559, https://doi.org/10.1016/j.infrared.2014.09.020.

[69] S. Surendra Babu, R. Rajeswari, K. Jang, C. Eun Jin, K. Hyuk Jang, H. Jin Seo, C. K. Jayasankar, Spectroscopic investigations of 1.06μm emission in Nd^{3+}-doped alkali niobium zinc tellurite glasses, J. Lumin. 130 (2010) 1021–1025, https://doi.org/10.1016/j.jlumin.2010.01.017.

[70] W.T. Silfvast, Laser Fundamentals, second ed., Cambridge University Press, United Kingdom, 2004.

[71] R. Jacobs, M. Weber, Dependence of the $^4F_{3/2} \rightarrow {}^4I_{11/2}$ induced-emission cross section for Nd^{3+} on glass composition, IEEE J. Quant. Electron. 12 (1976) 102–111, https://doi.org/10.1109/JQE.1976.1069101.

[72] L.A. Riseberg, M.J. Weber III, Relaxation phenomena in rare-earth luminescence, in: Progress in Optics, Elsevier, 1977, pp. 89–159, https://doi.org/10.1016/S0079-6638(08)70251-8.

[73] R. Rajeswari, S.S. Babu, C.K. Jayasankar, Spectroscopic characterization of alkali modified zinc-tellurite glasses doped with neodymium, Spectrochim. Acta Mol. Biomol. Spectrosc. 77 (2010) 135–140, https://doi.org/10.1016/j.saa.2010.04.040.

[74] Y. Chen, Y. Huang, M. Huang, R. Chen, Z. Luo, Effect of Nd^{3+} on the spectroscopic properties of bismuth borate glasses, J. Am. Ceram. Soc. 88 (2005) 19–23, https://doi.org/10.1111/j.1551-2916.2004.00009.x.

[75] K.U. Kumar, V.A. Prathyusha, P. Babu, C.K. Jayasankar, A.S. Joshi, A. Speghini, M. Bettinelli, Fluorescence properties of Nd^{3+}-doped tellurite glasses, Spectrochim. Acta Mol. Biomol. Spectrosc. 67 (2007) 702–708, https://doi.org/10.1016/j.saa.2006.08.027.

[76] A.R. Devi, C.K. Jayasankar, Optical properties of Nd^{3+} ions in lithium borate glasses, Mater. Chem. Phys. 42 (1995) 106–119, https://doi.org/10.1016/0254-0584(95)01564-7.

[77] S. Mohan, K.S. Thind, Investigation of luminescence and spectroscopic properties of Nd^{3+} ions in cadmium alkali borate glasses, Opt. Mater. 57 (2016) 134–139, https://doi.org/10.1016/j.optmat.2016.04.040.

[78] B. Shanmugavelu, V.V.R.K. Kumar, Luminescence studies of Dy^{3+} doped bismuth zinc borate glasses, J. Lumin. 146 (2014) 358–363, https://doi.org/10.1016/j.jlumin.2013.10.018.

[79] M.V. Vijaya Kumar, B.C. Jamalaiah, K. Rama Gopal, R.R. Reddy, Optical absorption and fluorescence studies of Dy^{3+}-doped lead telluroborate glasses, J. Lumin. 132 (2012) 86–90, https://doi.org/10.1016/j.jlumin.2011.07.021.

[80] R. Vijaya, V. Venkatramu, P. Babu, L.R. Moorthy, C.K. Jayasankar, 1.06 μm laser transition characteristics of Nd^{3+}-doped fluorophosphate glasses, Mater. Chem. Phys. 117 (2009) 131–137, https://doi.org/10.1016/j.matchemphys.2009.05.023.

[81] C.K. Jayasankar, R. Balakrishnaiah, V. Venkatramu, A.S. Joshi, A. Speghini, M. Bettinelli, Luminescence characteristics of Nd^{3+}-doped K–Ba–Al-fluorophosphate laser glasses, J. Alloys Compd. 451 (2008) 697–701, https://doi.org/10.1016/j.jallcom.2007.04.068.

[82] R.T. Karunakaran, K. Marimuthu, S. Arumugam, S. Surendra Babu, S.F. Leon-Luis, C.K. Jayasankar, Structural, optical absorption and luminescence properties of Nd^{3+} ions in NaO-NaF borate glasses, Opt. Mater. 32 (2010) 1035–1041, https://doi.org/10.1016/j.optmat.2010.02.026.